

MESON PRODUCTION AND MESON NUCLEUS INTERACTION STUDIES AT COSY*

H. MACHNER

Institut für Kernphysik, Forschungszentrum Jülich,
Postfach 1913, D-5170 Jülich, Germany

(Received January 27, 1995)

GEM is a detector with high spatial and energy resolution making it ideally suited for studies involving meson production close to threshold. The investigations proposed include study of the reaction mechanism of light mesons and their interaction with nuclei. In a first experiment the $p + p \rightarrow d + \pi^+$ reaction close to threshold was measured employing the magnetic spectrometer Big Karl together with dedicated detectors. A (preliminary) result is an anisotropy similar to the one in the time reversed reaction.

PACS numbers: 14.40.-n

1. Introduction

At COSY we aim to measure mesons close to threshold. This can be done with the help of the missing mass method. Suppose a two body reaction to occur, *i.e.* a reaction

$$A + B \rightarrow C + D \quad (1)$$

with A the projectile, B the target, C the unobserved meson and D the detected recoil particle. It is sufficient to measure only the properties of D like its energy, linear momentum, charge and baryon number for instance and deduce all corresponding quantities for C by applying the conservation laws. The precise measurement of the missing mass thus depends on the precise measurement of azimuth and polar angle.

A conventional accelerator delivers a particle beam with a certain beam diameter and a certain divergence. The situation for a large beam diameter

* Presented at the XXIX Zakopane School of Physics, Zakopane, Poland, September 5-14, 1994.

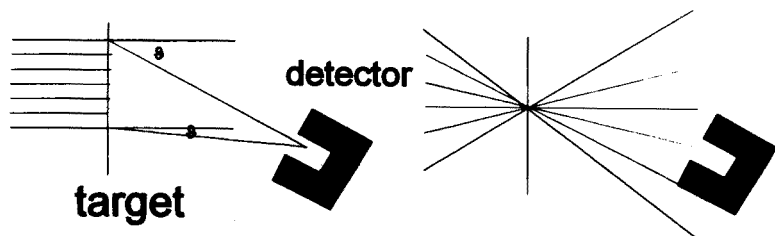


Fig. 1. Uncertainties in reaction angle measurements due to: (left part) a large beam diameter, (right part) a large divergence.

and a small detector element is sketched in the upper part of Fig. 1. Obviously, there is an uncertainty in the scattering angle depending on the spot size. Focussing to a smaller beam spot will not heal the problem, because of constant phase space the situation shown in the left part of the figure will arise with again an uncertainty in the scattering angle. One way out would be to introduce chambers measuring the trajectories of the incident particles. This will, however, limit the beam current and due to straggling in these detectors new ambiguities will be introduced. A better choice is the application of a phase space cooled beam, *i.e.* a beam with a very small diameter and very small divergence. Such beams will be delivered by COSY. Another uncertainty in the angle measurement can stem from the use of thick targets (compare Fig. 1). This is only a serious problem in the case of liquid gas targets. By development of a new liquid gas target we could reach thicknesses of 4 mm with still an excellent ratio of target nuclei to those in the windows [1].

GEM is a high resolution hybrid detector with large acceptance close to threshold. It will be described shortly in the following section. We will then describe the physics program of the GEM collaboration: study of the production of mesons in few body reactions and meson-nucleus interactions, especially in bound systems.

2. The GEM detector

The detector consists of the GErmanium wall and a Magnet spectrometer. The Germanium Wall is described in the contribution by Igel *et al.* [2]. It will allow the measurement of particles in an angular range larger than the acceptance of the magnet spectrometer BIG KARL. Particles being emitted in an inner cone will move through holes in the germanium diodes and will be detected by the magnet spectrometer. The Germanium Wall will deliver the following observables: polar angle and azimuth, energy loss and total energy. The latter two quantities yield the mass and charge of

the reaction product. From the mass and energy the linear momentum can be calculated yielding at the four momentum vector. For particles reaching the magnetic spectrometer the same quantities can be deduced. While the original design employed the so called parallel to point imaging, the magnet optics are presently changed with three new quadrupole magnets to an angle sensitive mode in the y-direction. It is, therefore, sufficient to measure the distance from the central plane in the y-direction. From the parallel to point imaging in the x-direction both the momentum and the emission angle can be determined by measuring the position in and the angle to the focal plane, respectively. This is done by two packets of multiwire-drift chambers (MWDC) which allow position measurements in x- and y-direction followed by four layers of scintillator paddles, acting as trigger hodoscopes and delivering energy loss signals and time-of-flight information as well. The set up of detectors in the exit of the magnet spectrometer is shown in Fig. 2.

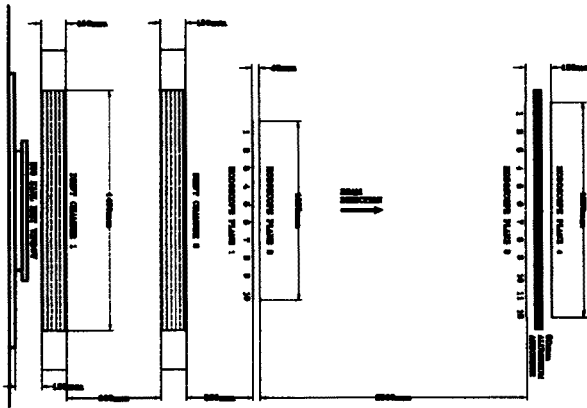


Fig. 2. Arrangement of detectors in the focal plane area of the magnet spectrometer.

3. Meson production

We will shortly discuss meson production close to threshold. As an example the two body kinematics of the $p+{}^2\text{H}\rightarrow{}^3\text{H}+\pi^+$ reaction is shown in Fig. 4 as a polar diagram in the reaction plane. The kinematical loci of ${}^3\text{H}$ and of π^0 then ellipses indicated by different curves for the beam momenta indicated in the figure. Also shown are acceptance limits of the GEM detector. The small angle opening indicated by dashed-dotted lines is the acceptance limit of the magnet spectrometer in x-direction. The solid lines indicate the angle acceptance of the Germanium wall. The solid curves

denote the maximum momentum of stopped ^3H particles in the different Germanium diodes: the quirl (ΔE) followed by calorimeter crystals ($E_{1,2}$). As one can see from this figure GEM has for the ^3H particles an acceptance of 100 spatial as well as momentum acceptance for beam momenta below 950 MeV/c. It is therefore ideally suited for the complete measurement of cross sections. Because of its rotational symmetry it can also measure analyzing powers if a polarized beam is used.

Why should one study this long known reaction at all? One argument among others is the paucity of data in the region close to threshold. One can expect in this area nonresonant contributions to the cross section to dominate in comparison with the Δ -resonance. In addition, two step processes may contribute at backward angles [4]. In Fig. 3 we compare differential cross sections from different experiments.

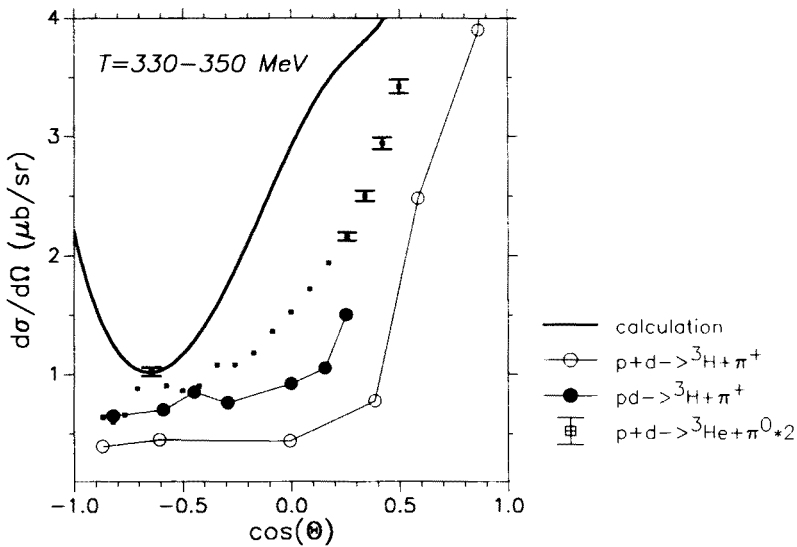


Fig. 3. Differential cross section as function of the cosine of the emission angle in the center of mass system. The different reactions are indicated in the figure.

4. Meson-nucleus interactions

The hadronic interaction between mesons and nuclei is barely known. A very sensitive tool to study these interactions is the investigation of bound mesic states. Such systems are known in the case of π^- as pionic atoms. The classical method, the study of transitions between atomic levels by detection of emitted γ -rays, fails when approaching states in the vicinity of the nuclear surface, because of the strong interaction leading to annihilation. However, it is just this interaction which is of interest. We, therefore, proposed [3]

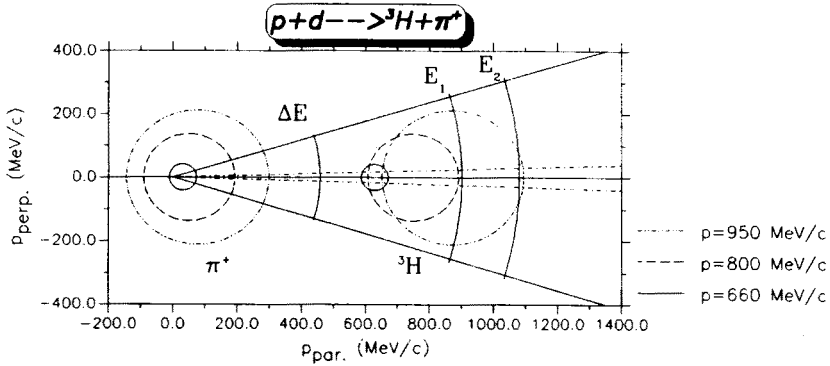


Fig. 4. The kinematical loci of π^+ and ^3H -nuclei are shown in a polar diagram as function of the momenta parallel and perpendicular to the beam axis.

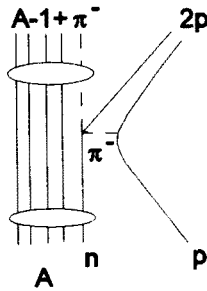


Fig. 5. Graph of the production of a π^- in a bound state.

an alternative approach. We plan to produce the pionic atom by production of a pion directly in this bound state. This reaction is sketched in Fig. 5. The cross section for such a reaction is given in the impulse approximation by

$$\frac{d\sigma(p + A, A - 1 + \pi^- + 2p)}{d\Omega} = \frac{d\sigma(p + n, 2p + \pi^-)}{d\Omega} \times \left| \int \varphi_f e^{-\frac{i}{\hbar} \vec{r}(\vec{p}_f - \vec{p}_i)} \varphi_i d^3r \right|^2. \quad (2)$$

The first factor on the right hand side is the cross section for the elementary process while the integral contains the wave functions of the initial and final systems and the linear momentum transferred in the exponential. The elementary cross section will raise close to threshold as $p_{\pi, \max}^{(2l+1)}$ with l denoting the partial wave quantum number. Evidently, this factors raises slower than the exponential drops down. The maximum for the integral is obtained for

$\vec{p}_f - \vec{p}_i = 0$, which means, that the two emerging protons carry all beam momentum.

There have recently been attempts to make use of reactions similar to this in Fig. 5. Iwasaki *et al.* [5] made use of the $n + {}^{208}\text{Pb} \rightarrow {}^{207}\text{Pb} + \pi^-$ reaction at 418 MeV which corresponds to a momentum transfer of ≈ 40 MeV/c. The experiment suffered from poor statistics and a resolution of 1.15 MeV. An improved run yielded a bump of on a smooth background of $300 \mu\text{b}/(\text{MeV sr})$ [6]. However, even that statistics and energy resolution did not allow to identify individual lines. The same is true for a $(p, 2p)$ experiment on ${}^{208}\text{Pb}$ with 0.8 MeV energy resolution [7]. In order to get an estimate on the energy resolution required we extrapolate the existing data on the $1s_\pi$ -level width. This is shown in Fig. 6. The corresponding shifts due to the strong interaction is also shown for completeness. A simple extrapolation to $A = 208$ yields a width of 6 MeV. If that would be true no lines could be measured. However, Toki *et al.* [8] gave by applying a Kisslinger type potential a value $\Gamma_{1,s}({}^{208}\text{Pb}) = 632$ keV. In a new parametrization of the potential parameters Konijn *et al.* [9] found a saturation effect with a width of only 118 keV. For ${}^{40}\text{Ca}$ the two results are 105 keV and 95.3 keV, respectively. This is still in agreement with the extrapolation shown in the figure. One goal of the detector development was therefore to reach a resolution better than 100 keV. First results are encouraging [2].

The study of the η -nucleus interactions is planned along similar paths. Details of that proposal are given elsewhere [10]. There also the proposed studies of light mesons close to threshold are discussed. We will concentrate now on the first experiments performed with only the magnet spectrometer.

5. Meson production experiments

5.1. Motivation for the chosen reaction

The reaction $p + p \rightarrow d + \pi^+$ is well studied in the region of the Δ -resonance and down to a pion momentum $\eta (= p_{\text{cm}}^\pi/m_\pi) \approx 0.9$ [11]. There is a serious lack of data down to threshold. In this momentum range only cross sections and asymmetries from the time reversed reaction $\pi^+ + d \rightarrow p + p$ and the isospin related reaction $n + p \rightarrow d + \pi^0$ exist [12–14]. Korkmaz *et al.* [15] have measured only analyzing powers in this regime. It is our aim to complete the cross section measurements close to threshold. Because of the two body final state it should be a not to complicated reaction, thus allowing to study the detector response as well.

5.2. Experiment

The experiment was carried out at the COSY accelerator at Jülich. The beam properties were as follows: spot with $\text{FWHM} < 2$ mm, $5 \cdot 10^6$ protons

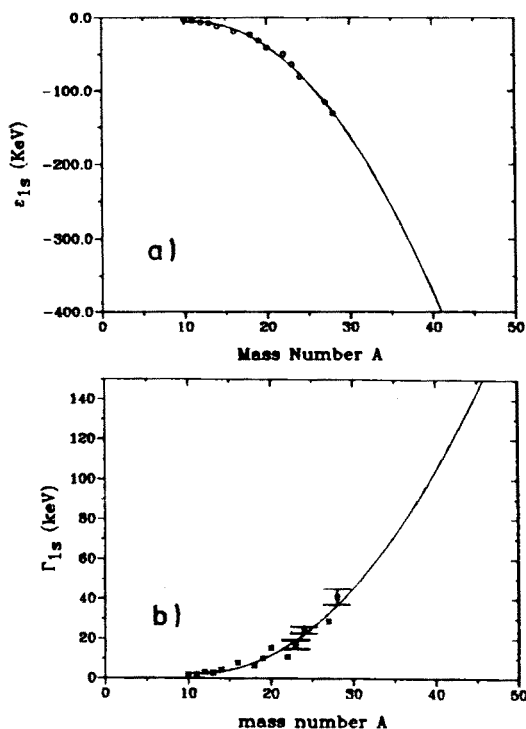


Fig. 6. Compilation of measured shifts (a) and widths (b) of pionic 1s states for $N = Z$ nuclei with $Z = \text{odd}$.

per spill with a duration of 1 second and a repetition of every 5 seconds. The detector set up is dictated by the underlying kinematics. Close to threshold even a detector with limited acceptance can be used as a 4π -detector. A serious problem is that beam momentum and momenta of the recoiling deuterons are quite similar. Hence, the beam particles will either appear in the focal plane or, when stopped in some beam dump, produce a large background in the focal plane. By choosing the second option we have decided to dump the beam at the exit of the second dipole magnet of BIG KARL into the side yoke. To reduce the enormous background we used a ring shaped scintillator behind the target to detect the pions and to give a start signal for the time of flight measurement through the spectrometer (≈ 15.5 m flight path). The track of reaction products was measured in the focal plane area with two stacks of Multi-Wire Drift Chambers (MWDC), each consisting of six layers. They were 60 cm apart of each other and allow the measurement of the position in x- and y-direction. These chambers were followed by four layers of scintillators serving as trigger hodoscopes. The first two layers consisted of ten individual scintillator paddles each, two

stacked ones operating in coincidence. The second layer produced also the stop signal for the time-of-flight measurement. The third and fourth layer consisted of twelve paddles each. Between these two layers an aluminum absorber was mounted with thickness sufficient to stop the deuterons but allowing protons with momenta close to the beam momentum to penetrate. While the signal in the third layer was used as another coincidence signal, events in the fourth layer delivered veto signals. In order to define the beam spot precisely we have used another ring scintillator in front of the target with 3 mm diameter. In summary: the trigger enabling the data acquisition was a coincidence between a possible deuteron measured in the focal plane and a pion measured in the ring detector behind the target vetoed by the beam-defining ring.

The target was a cell of 4 mm thickness and 5 mm diameter containing liquid hydrogen [1]. The windows were made from Mylar of $1.5\ \mu\text{m}$ thickness.

5.3. Results

A time of flight spectrum measured as described above is shown in the left part of Fig. 7. It is clearly dominated by protons having momenta almost equal to the beam momentum. When in addition gates are set on the Δ -E spectra measured in the hodoscope to particles with large energy loss, the TOF spectrum in the right part of Fig. 7 is obtained. This spectrum

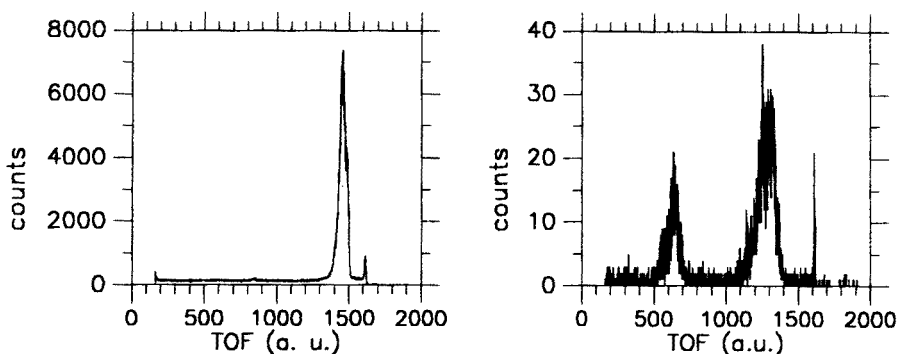


Fig. 7. Left part: raw TOF spectrum according to trigger conditions discussed in the text. Right part: reduced TOF spectrum with gates selecting large energy losses in the hodoscope scintillators.

clearly shows two distinct groups: at the right side protons with lower momenta than the beam but still in the acceptance of the spectrometer and at the left side particles with half the beam velocity, *i.e.* recoiling deuterons. We then sorted data under the additional constraint to lie in this group.

From the particle track measured in the focal plane we then reconstructed the emission vertex of the deuterons. The results of this analysis is shown in Fig. 8 as contour plot. Obviously, there is a spread in the data according to the kinematical curves also shown. This may correspond to different beam momenta. Such a spread in momenta is expected for the resonance extraction presently employed. The uncertainty of 0.5 % corresponds to the geometrical acceptance of COSY.

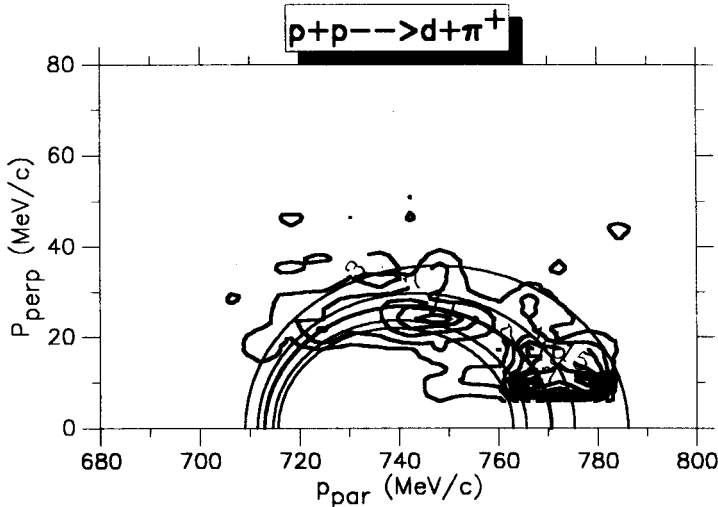


Fig. 8. Reconstructed deuteron momenta from the indicated reaction are shown as contour plot. Also shown are kinematic loci for beam momenta 795, 796, 798, 800, 805 MeV/c, respectively.

We proceed by interpolating the data along the kinematic locus prescribed by a beam momentum of 798 MeV/c and projecting the data onto the x-axis. The resulting distribution can be converted directly into a center-of-mass angular distribution shown in Fig. 9. Also shown is the acceptance of the whole set up for a monoenergetic beam with zero diameter. It can be seen that the angular distribution is affected to a large extent by the acceptance limits. Monte Carlo studies including the finite size of the beam spot are presently been carried out. The finite size of the beam spot will wash out the sharp edges in the acceptance limits. We can then fit Legendre polynomials with coefficients a_i to the angular distribution. First estimates yield for $\eta = 0.20$ an anisotropy $a_2/a_0 = 0.27 \pm 0.02 \pm 0.09$ for which the errors represent systematic and statistical uncertainties, respectively. This value is compared with previous values for the same reaction, the time reversed and isospin related reactions in Fig. 10. Close to threshold only s - and p - wave should contribute to the cross section. The first partial wave is believed to account for non resonant rescattering while p -wave should

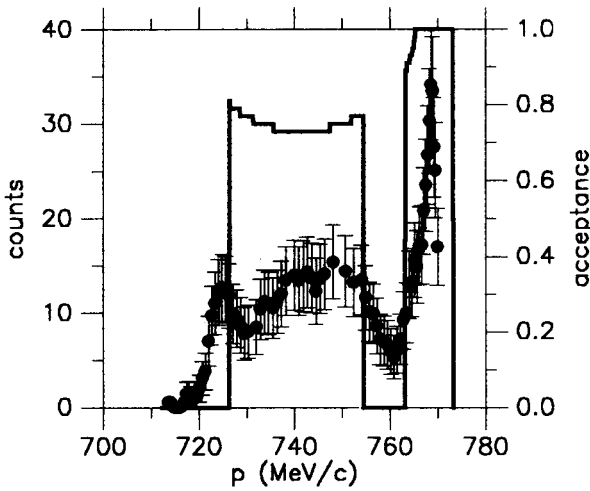


Fig. 9. Angular distribution of deuterons (*preliminary*) in the center of mass system for a beam momentum of 798 MeV/c (dots with error bars). The acceptance probability of the detector set up for a point like beam spot is shown as histogram.

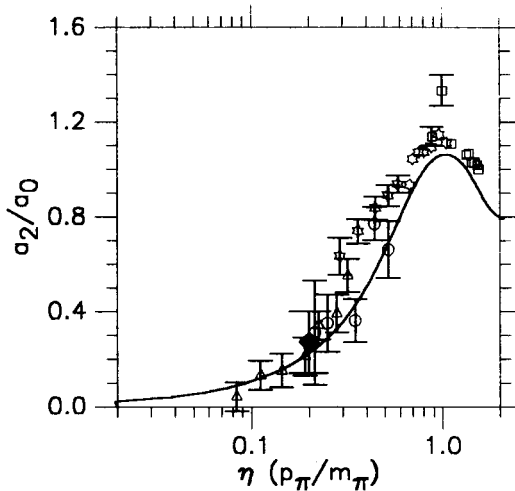


Fig. 10. Anisotropies as function of the pion cm-momenta relative to the pion mass. Experimental results are shown by symbols with error bars (Jones (compilation) as open squares, present *preliminary* data as full diamond, time reversed reaction as measured by Ritchie *et al.* by open dots, neutron induced reactions: Hutcheon *et al.* by open triangles and Roessle by open stars) together with a calculation performed by Niskanen as curve.

represent the influence of the production through the Δ -resonance. A calculation performed by Niskanen [16] taking these two processes into account is shown in the figure as well.

6. Discussion

The GEM detector is presented. We show that it is an ideal tool to study meson production and meson nucleus interactions close to threshold. Proposed studies of meson-nucleus interactions are discussed on the example of negatively charged pions. These may form a bound state (pionic atoms). We have shown that the modernized spectrometer together with its new focal plane detectors will allow us to measure differential cross sections of pion production close to threshold. A deduced anisotropy is in agreement with those from related reactions in the momentum range of interest. In order to extract absolute cross sections the monitoring of the incident beam intensity is required more accurately. The set up is currently being improved with respect to the acceptance probability. By using a smaller beam spot and an ever thinner target we will be able to measure even closer to threshold.

Note added in proof: After completion of this manuscript we performed a new measurement with an improved set up. This resulted in a much larger body of data with higher quality.

REFERENCES

- [1] V. Jaeckle *et al.*, *Nucl. Instrum. Methods Phys. Res.* **A349**, 15 (1994).
- [2] S. Igel *et al.*, *Acta Phys. Pol.* **B26**, 627 (1995).
- [3] H. Machner *et al.*, COSY proposal 10 (1991).
- [4] K. Kilian, H. Nann, *Particle Production Near Threshold*, AIP Conference Proceedings No. 221, 185 (1990).
- [5] M. Iwasaki *et al.*, *Phys. Rev.* **C43**, 1099 (1991).
- [6] A. Trudel *et al.*, TRIUMF Annual report 1991.
- [7] N. Matsuoka *et al.*, in H. Machner and K. Sistemich Eds., *Proc. Int. Conference with GeV particle beams*, Jülich 1994, World Scientific, Singapore, in press.
- [8] H. Toki *et al.*, *Phys. Lett.* **B213**, 129 (1988); *Nucl. Phys. A* **501**, 653 (1989).
- [9] J. Konijn *et al.*, *Nucl. Phys.* **A519**, 773 (1990).
- [10] H. Machner *et al.*, *Acta Phys. Pol.* **B24**, 1555 (1993).
- [11] G. Jones, in R. D. Bent (Editor), *Pion Production and Absorption in Nuclei-1981*, AIP Conference proceedings 79, 15 (1982).
- [12] B. G. Ritchie *et al.* *Phys. Rev. Lett.* **66**, 568 (1991); *Phys. Rev.* **C44**, 533 (1991).

- [13] E. Rössle, in Ref. [11]
- [14] D. A. Hutcheon *et al.*, *Phys. Rev. Lett.* **64**, 176 (1990).
- [15] E. Korkmaz *et al.*, *Nucl. Phys.* **A535**, 627 (1991).
- [16] J. A. Niskanen, *Nucl. Phys.* **A298**, 417 (1978).